Available online at www.sciencedirect.com
ScienceDirect
Journal of Nuclear Materials 363–365 (2007) 1450–1456
journal of nuclear materials
www.elsevier.com/locate/jnucmat

Surface temperature measurements by means of pulsed photothermal effects in fusion devices

Th. Loarer [a,*], F. Brygo [b], E. Gauthier [a], C. Grisolia [a], F. Le Guern [b], F. Moreau [a], A. Murari [c], H. Roche [a], A. Semerok [b]

[a] Association EURATOM-CEA, DSM-DRFC, CEA Cadarache, 13108 Saint Paul lez Durance, France
[b] CEA Saclay, DEN-SAC-DPC-SCP-LILM, 91191 Gif sur Yvette, France
[c] Associazione EURATOM-ENEA per la Fusione, Consorzio RFX, 4-35127 Padova, Italy

Abstract

In fusion devices, the surface temperature of plasma facing components is measured using infrared cameras. This method requires a knowledge of the emissivity of the material, the reflected and parasitic fluxes (Bremsstrahlung). For carbon, the emissivity is known and constant over the detection wavelength (~3–5 μm). For beryllium and tungsten, the reflected flux could contribute significantly to the collected flux. The pulsed photothermal method described in this paper allows temperature measurements independently of both reflected and parasitic fluxes. A local increase of the surface temperature ($\Delta T \sim 10$–15 K) introduced by a laser pulse (few ns) results in an additional component of the photon flux collected by the detector. Few μs after the pulse, a filtering of the signal allows to extract a temporal flux proportional only to the variation of the emitted flux, the emissivity and ΔT. The ratio of simultaneous measurements at two wavelengths leads to the elimination of ΔT and emissivity. The range of application increases for measurements at short wavelengths (1–1.7 μm) with no limitation due to the Bremsstrahlung emission.

1. Introduction

In most of the existing tokamaks, the plasma facing components are in carbon, allowing large temperature excursions without any dramatic and irreversible damages. However, in future fusion devices, to alleviate the problem of tritium retention, carbon will be limited to the strict minimum and likely replaced by metallic materials. In these conditions of metallic environment, the power handling capability of the plasma facing components (PFC) (mainly divertor and first wall) in both steady state and fast dynamic heat deposition events (ELMs, disruption...) is of a major issue. For next step fusion devices, such as ITER, the reference scenario of ELMy H-mode with type I ELMs is of a particular concern. The ITER-like wall project [1] of JET with a full metallic machine (first wall in Be and divertor in W) will require a careful control of the plasma scenario in terms of plasma wall interactions associated with reliable surface temperature measurement techniques in this high reflectivity and parasitic environment.

* Corresponding author.
E-mail address: thierry.loarer@cea.fr (Th. Loarer).

0022-3115/$ - see front matter © 2007 Published by Elsevier B.V.
doi:10.1016/j.jnucmat.2007.01.205

In today fusion devices, the surface temperature of the target plates is generally measured using an infrared camera. This is a robust and well known method widely used in tokamaks for surface temperature analysis [2–4] with carbon as main plasma facing components since the carbon emissivity is generally always high (>0.8) and also independent of the plasma conditions. This method is also used for safety considerations to limit and avoid the possible damages of the plasma facing components in case of too intense heat load [2]. The development of techniques using optic-fibres to estimate the surface temperature has also been carried out and have shown that, for opaque materials, the surface temperature can be estimated [5], assuming a uniform temperature profiles on the viewed area, by each fibre. Other methods have also been considered, like measuring at two and even three wavelengths [6], to take into account the possible variation of the emissivity over the detection range. However, for all of these methods, it is assumed that the reflected flux contribution to the collected flux is negligible. This is generally correct since the observations nearly always concern the hottest area with a high emissivity. With metallic walls, the emissivity of these PFCs is lower at least by a factor of two compared to carbon and/or exhibits variations over both the temperature and wavelength detection ranges. In these experimental conditions, the reflected flux will contribute to a non-negligible part of the flux collected by the detector and for the outer wall, this contribution will be very likely larger than the emission due to its low surface temperature. The modelling of the multiple reflections could be carried out, but, contrary to the industrial furnaces with steady state conditions [7], in time varying tokamak conditions, the assessment of temperature measurements can be very difficult and not reliable in terms of safety during fast dynamic events. As a consequence, if the reflected and parasitic fluxes cannot be removed from the total signal, the classical IR thermography, relying on a collected flux solely resulting from the emitted flux, cannot be used to measure correctly the true surface temperature of the viewed area.

In this paper, a pulsed photothermal method is proposed allowing the surface temperature to be measured without error due to reflected fluxes from surrounding surfaces [8,9] and also from parasitic emission from the plasma like Bremsstrahlung. In this method, a pulsed laser (few ns) induces a local surface temperature variation. The resulting temporal increase of the emitted flux is proportional to the surface temperature variation and independent from both the reflected flux and the parasitic emission assumed to remain constant over the heat pulse duration and few μs after the laser pulse. The radiation collected by the detector results from the sum of a constant term (emission, reflection and parasitic flux) and a dynamic term (variation of the emission). The separation of these two components can be performed using a filtering of the signal. The surface temperature can be deduced from the dynamic term since it depends on three unknowns: the surface temperature of the target, its emissivity and the dynamic component of the surface temperature introduced by the laser pulse. The ratio of two simultaneous measurements at two different wavelengths is performed to eliminate the surface temperature induced by the heat pulse. The resulting ratio of the emissivities at these two wavelengths can be estimated either at a known temperature (before the plasma breakdown, for example) or by assuming a known ratio. An essential feature of this technique is that changes in emissivity, parasitic fluxes and/or of the temperature of the environment over timescales larger than typically 10 μs do not introduce any errors in the surface temperature determination.

The theoretical considerations of the pulsed photothermal method applied to the surface temperature measurement are discussed in the first section. The principle of the surface temperature measurement is presented in the second section. The temperature and wavelength ranges of the method in the environment of a tokamak and in the frame of the project of a metallic wall are discussed in the last section.

2. Theoretical considerations

The photon flux collected at a wavelength λ by a detector viewing a solid surface of an opaque material at temperature T_o, in a surrounding assumed to be at temperature T_s and exposed to a plasma flux can be described by its radiance L_λ^e and written in the form:

$$L_\lambda^e = \varepsilon'_\lambda L_\lambda^0(T_o) + (1-\varepsilon'_\lambda)L_\lambda^0(T_s) + L_\lambda^{Brem}, \quad (1)$$

where L_λ^0 stands for the blackbody radiance, ε'_λ for the spectral directional emissivity and L_λ^{Brem} for the Bremsstrahlung emission of the plasma located between the target and the detector.

Only the first term on the right hand side, the emitted radiance, depends on the temperature of

the sample, but a detector cannot separate the emitted flux from the reflected flux and the parasitic flux. In case of high emissivity, when $T_o > T_s$, classical pyrometry can be used by assuming that both the reflected and parasitic fluxes give negligible contributions to the collected signal. However, when these experimental conditions are not fulfilled, the difference between estimated temperature and the true temperature can be very high. Fig. 1 shows the values of the temperature T_m which would be deduced from a monochromatic pyrometer assuming that the spectral emissivity is known but without considering a contribution from the reflected flux and with a Bremsstrahlung emission which is negligible at 3 μm (see below). As it can be seen from this figure, when the emissivity of the observed target is higher than about 0.7, the effect of the reflected flux at 3 μm is in the order of 18–25% provided the surrounding temperature, T_s, remains less than 1200–1400 K. However, for emissivities lower than 0.3, the contribution of the reflected flux in the collected flux leads to very high errors. Indeed, for a surrounding temperature of 'only' 1200 K and a real surface temperature of 1000 K, the temperature is estimated to be 1600 K. It is worth noting that for longer wavelength this error is even higher and at 5 μm a temperature of 2200 K would be estimated. This is due to the lower contribution of the emitted flux at 1200 K at 5 μm compared to the intensity at 3 μm.

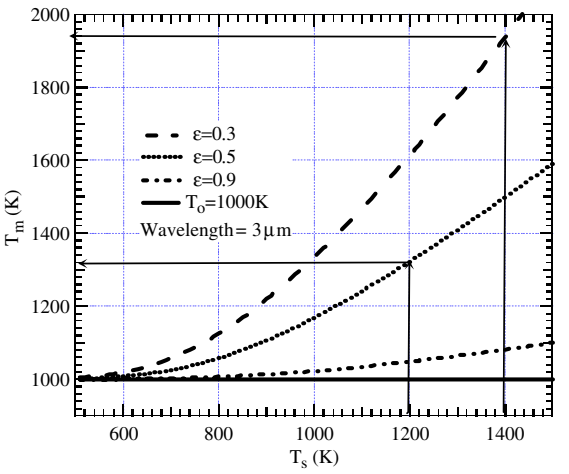

Fig. 1. Influence of the reflected flux on the measured surface temperature T_m, by classical pyrometry given by $L_\lambda^0 = \varepsilon'_\lambda L_\lambda^0(T_m)$ assuming that all the collected flux is the emitted flux. The target is at a temperature $T_o = 1000$ K located in a surrounding at a temperature of T_s. Three target emissivities are considered, the detection wavelength is taken at 3 μm and the Bremsstrahlung emission is neglected.

In tokamaks, optical pyrometry can be used only when $\varepsilon'_\lambda L_\lambda^0(T_o) \gg (1-\varepsilon'_\lambda)L_\lambda^0(T_s) + L_\lambda^{Brem}$. In today's tokamaks, where carbon is used to handle high heat flux on the target plates of the divertor, the emissivity is >0.8. As a consequence, the contribution of the term $(1-\varepsilon'_\lambda)L_\lambda^0(T_s)$ in the total signal remains weak. The Bremsstrahlung emission L_λ^{Brem} becomes significant for short detection wavelengths (<1 μm) and can therefore significantly contributes to the collected signal in short detection wavelength range. Fig. 2 shows the ratio $R(\lambda, T_o) = \frac{L_\lambda^0(T_o)}{L_\lambda^0(T_o)+L_\lambda^{Brem}}$ as a function of T_o for different detection wavelengths for a central density of $n_e(0) = 6.0\times10^{19}$ m^{-3}, a central temperature of $T_e(0) = 5$ keV, parabolic profiles and a minor plasma radius of 0.8 m. It can be seen that for temperature lower than typically 1000 °C and in the detection range 0.7–0.9 μm, the contribution of the Bremsstrahlung emission can be significant. It is worth noting that the Bremsstrahlung emission increases proportionally to $n_e T_e^{1/2}$ showing that this contribution increases with the plasma performances. Working at long wavelengths (>5 μm) for detection represents the advantage of nearly no contribution from both Bremsstrahlung and hot spots. However, the contribution of the emissivity increases and in the case of strong variation of the emissivity (for example, when beryllium melts, the emissivity drops from about 0.5 to only 0.1) this can lead to huge errors. Working at short wavelengths allows to strongly reduce the impact of the emissivity in the signal but as shown above the Bremsstrahlung emission becomes non-negligible. However, it is worth noting that independently

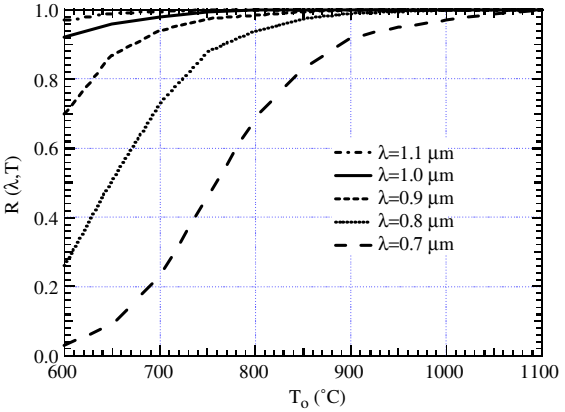

Fig. 2. Ratio $R(\lambda, T_o) = \frac{L_\lambda^0(T_o)}{L_\lambda^0(T_o)+L_\lambda^{Brem}}$ as a function of T_o for different detection wavelengths for a central density of $n_e(0) = 6.0\times10^{19}$ m^{-3}, a central temperature of $T_e(0) = 5$ keV.

of the wavelength range, the contribution of the reflected flux remains.

In future fusion devices, the carbon will be replaced by metallic walls; Be for the wall and W for the divertor in the case of the JET-EP2 project [1] while the plasma performances should be improved also leading to an enhanced neutron flux. The actual methods to measure the surface temperature are based on IR measurement integrated over the 3–5 μm wavelength range [2–4] but the use of the classical IR camera detection could be compromised not only by the neutrons (not discussed in this paper) but also by the reflected and by the parasitic fluxes particularly if short detection wavelengths (CCD camera for example) are used. The pulsed photothermal method is used to separate the emitted flux from the collected flux and therefore to deduce the true surface temperature independently of the reflected and parasitic fluxes. This method has been developed both in modulated and pulsed regimes [8,9] and applied for the surface temperature measurement of wings in industrial turbines [10] (strong reflected flux between fixed and moving wings) and for further developments with optical fibres [11].

3. Principle of the surface temperature measurement

In tokamak's experimental conditions, the emitted, reflected and parasitic fluxes can be assumed constant over a duration of 10–20 μs. The local perturbation $\Delta T(r,t)$ of the temperature introduced by means of a pulsed local illumination results in a local temperature which can be written as $T(r,t) = T_o + \Delta T(r,t)$. If $\Delta T(r,t) \ll T_o$ (10 K compared to 1000 K) and the variation of the emissivity over this temperature variation can be considered negligible, the flux leaving the target is proportional to the following expression:

$$\Phi_\lambda(t) \propto \varepsilon'_\lambda L^0_\lambda(T_o) + (1-\varepsilon'_\lambda)L^0_\lambda(T_s) + L^{\mathrm{Brem}}_\lambda + \varepsilon'_\lambda \frac{\partial L^0_\lambda}{\partial T}(T_o)\Delta T(t). \quad (2)$$

Therefore, the radiation leaving the target appears to be the sum of a continuous term and a dynamic term. The continuous term contains the emitted flux, the reflected flux and the parasitic emission. The dynamic term only depends on the temperature derivative of the radiance, temperature variation and its associated emissivity. Therefore, by filtering the electric signal delivered by the detector, it is possible to separate the continuous from the dynamic components and consequently to separate the reflected, emitted and parasitic fluxes from a term which only depends on the emitted flux.

The dynamic photothermal signal collected by a detector depends on three unknown parameters: the derivative of the radiance with respect to the temperature T_o, the emissivity ε'_λ, and the dynamic component of the surface temperature, $\Delta T(t)$, introduced by the laser pulse. For a given wavelength of detection, this signal $S_\lambda(t)$ can be written in the form [8,9]:

$$S_\lambda(t) = D_\lambda \varepsilon'_\lambda \Delta\Omega \tau_\lambda \Delta\lambda \frac{\partial L^0_\lambda}{\partial T}(T_o) \int_{\Delta S} \Delta T(t)\,\mathrm{d}S, \quad (3)$$

where D_λ is the detectivity of the detector, $\Delta\Omega$ the solid angle of the detection, τ_λ the transmission factor of the overall measurement chain, $\Delta\lambda$ the spectral bandwidth of the detection and ΔS the area viewed by the detector.

With mixed materials already used in ASDEX [12] and foreseen in JET [1] and in ITER [13], the emissivity will be in the range 0.2 to 0.8–1.0 depending on the material and also on the possible deposited layers on the PFCs. Therefore, the emissivity has to be estimated from the chain of measurement. $\Delta T(t)$, has to be eliminated since this value cannot be determined with sufficient accuracy.

To eliminate $\Delta T(t)$, two simultaneous measurements at two wavelengths, λ_1 and λ_2, can be performed and by making the ratio of theses signals, the following expression results:

$$\frac{S_{\lambda_1}}{S_{\lambda_2}} = \left(\frac{D_{\lambda_1}\tau_{\lambda_1}\Delta\lambda_1}{D_{\lambda_2}\tau_{\lambda_2}\Delta\lambda_2}\right)\frac{\varepsilon'_{\lambda_1}}{\varepsilon'_{\lambda_2}}\frac{\frac{\partial L^0_{\lambda_1}}{\partial T}(T_o)}{\frac{\partial L^0_{\lambda_2}}{\partial T}(T_o)}. \quad (4)$$

In this expression, it can be seen that the geometrical factor $\Delta\Omega$ has also disappeared while the first ratio of the right hand side of Eq. (4) can be determined by an appropriate calibration procedure. The ratio of the emissivities also results and it has to be eliminated to extract T_o. The problem of the emissivity can be overcome using the so-called two colour approximation, in which it is assumed that the ratio $\varepsilon'_{\lambda_1}/\varepsilon'_{\lambda_2}$ is known and/or equal to unity. An other possibility is to work at short wavelengths as discussed in the following section.

4. Characteristic time and detection wavelength

This part focuses on the analysis of the time evolution of the photothermal signal collected by

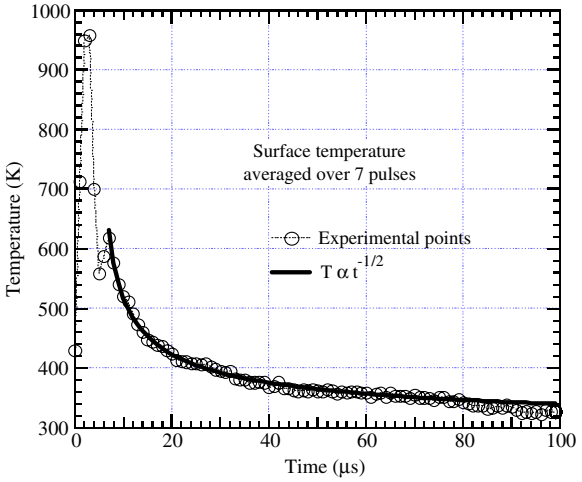

Fig. 3. Time evolution of the surface temperature of a graphite tile of Tore Supra during a series of laser pulse. The fluence of the laser heat pulse is $= 0.7\ \mathrm{J/cm^2}$, the repetition rate is 10 kHz, the laser wavelength is 532 nm and the pulse duration is 90 ns. This signal represents the averaged of the sum of seven consecutive pulses to analyse the characteristic times.

a pyrometer during a series of laser pulses carried in a laboratory on a graphite tile removed from the tokamak Tore Supra (Fig. 3). The fluence of each heat pulse is $0.7\ \mathrm{J/cm^2}$, the repetition rate is 10 kHz, the laser wavelength is 532 nm, the pulse duration is 90 ns and the detector is a 'Pyroskop 274-LWL' (1.58–2.2 μm of detection range) with a time response of 10 μs. In this example, the amplitude of the thermal perturbation is very high compared to what would be necessary for the pulsed photothermal method where 10 K is large enough to get a significant signal to noise ratio. The surface temperature variation is proportional to the energy density deposition of the heat pulse. A lower energy would 'simply' lead to a lower signal amplitude and an increase of the illuminated area would also lead to a drop of the amplitude, but in this case, the space resolution would be affected.

Three phases can be distinguished from this plot. The first phase occurs immediately after the heat pulse and range from 0.09 μs to 7 μs. The peak observed on the temperature results from hot spots due to the energy deposition on a non-uniform surface and therefore leading to locally very high temperature. This phenomenon is similar to what is observed during plasma wall interaction on carbon [14]. This phase is difficult to use for surface temperature measurement since the 'information' of the surface temperature is not easy to extract from this part of the photothermal signal. Indeed, the signal intensity clearly results from the contribution of the non-uniform surface temperature (local hot spots) and possibly from dusts. The two following phases, respectively from 7 to 80 μs and above 80 μs, exhibit a time evolution, respectively, proportional to $t^{-1/2}$ and $t^{-3/2}$. These two time evolutions can be explained by the area observed compared to the area heated (diameter ~1 mm) by the laser. In the first phase ($t^{-1/2}$), the heat diffusion on the observed area (diameter of 0.5 mm) takes place only in depth and can be assumed as the classical semi-infinite modelling. The observed area is smaller than the characteristic length of heat diffusion in the radial direction, w^2/D where w is the laser beam waist and D the thermal diffusivity. After 80 μs, the diffusion process over the radial direction is also observed and the time constant evolves as $t^{-3/2}$. In terms of time resolution, this example clearly shows that a synchronised acquisition of the signal between 7 and 10 μs after the laser pulse would allow measurements without any contribution from hot spots, reflected and parasitic fluxes. During this width of 3 μs, the plasma conditions (Bremsstrahlung) and the reflected flux can be supposed constant. The signal acquisition over 1 μs in this window is short enough to envisage a time resolution for the power ELM deposition. In terms of time constant, the limitations of the method come both the transient hot spots (<1 μs [14]) induced by the laser pulse (non-uniform surface temperature) and of the assumption that in the time window between the laser pulse and the final detection the surrounding remains in steady state even during ELMs and sawteeth, for example.

If the emissivity is not well known at short detection wavelength, the effect on the resulting temperature deduced either by monochromatic pyrometry and/or photothermal pyrometry leads to a weak error as the wavelength of detection is decreased. Also, it is worth noting that with classical pyrometry strong variations of the emissivity can lead to very large errors in the temperature estimation. As an example, during High Heat Flux (HHF) testing on beryllium in JET Test Bed it was found [15] that with increasing surface temperature the emissivity increases (from ~0.3 up to ~0.5–0.6) but that immediately after melting (~1200 °C) the surface becomes very clean and the emissivity drops dramatically to values as low as 0.1. With classical pyrometry, such a decrease of the collected signal by a factor of 5 could be interpreted as a result of

a lower surface temperature. Since the emissivity ratio does not change in this huge proportion the photothermal method would clearly lead to a more precise estimation of the surface temperature. In addition, working at short wavelength also strongly reduce the error associated to a variation of the emissivity ratio as shown below.

Fig. 4 shows the ratio of the signals (Eq. (4)) plotted as a function of the temperature for two wavelength $\lambda_1 = 1.1$ μm and $\lambda_2 = 1.6$ μm and for two ratio of the emissivities $\varepsilon_{\lambda_1}/\varepsilon_{\lambda_2} = 1$ and $\varepsilon_{\lambda_1}/\varepsilon_{\lambda_2} = 0.75$. The same ratio is plotted for a pair of wavelengths in the IR detection bandwidth $\lambda_1 = 3.0$ μm and $\lambda_2 = 5.0$ μm. From this figure it can be seen that the effect of an error on the ratio of the emissivities is also significantly reduced for short wavelengths while the signal ratio exhibits a wider dynamic as a function of the temperature. Indeed, an error of 25% on the emissivity ratio leads to a maximum error of 200 K for a temperature of 2000 K at $\lambda_1 = 1.1$ μm and $\lambda_2 = 1.6$ μm. while it would be of 600 K for $\lambda_1 = 3.0$ μm and $\lambda_2 = 5.0$ μm.

InGaAs CCDs detectors work in the 1.1–1.6 μm range and can cover a temperature range from 300 to 2000 °C by adjusting the exposure time and/or by using natural filters for higher temperature. This could also permit to work with 'ordinary' glass optics at 1.6 μm. Even if no discussed in this paper, it is worth noting that the noise resulting from neutrons is also significantly less compared to the InSb detectors more traditionally used in the 3–5 μm range and also that the price of these detector is significantly lower than the InSb detectors.

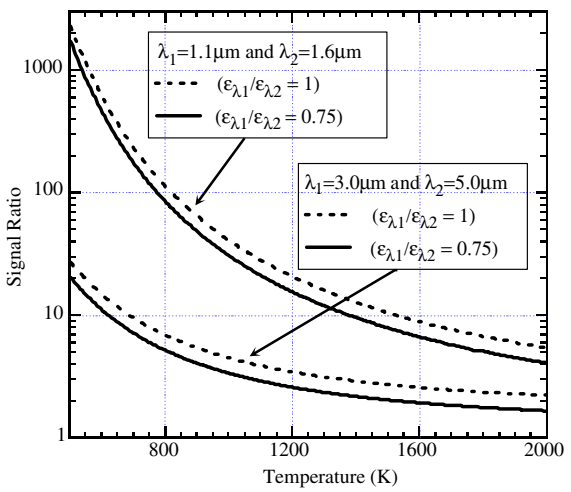

Fig. 4. Ratio of the photothermal signals plotted as a function of the surface temperature for two sets of wavelengths ($\lambda_1 = 1.1$ μm and $\lambda_2 = 1.6$ μm) and ($\lambda_1 = 3.0$ μm and $\lambda_2 = 5.0$ μm) and for two ratio of the emissivities $\varepsilon_{\lambda_1}/\varepsilon_{\lambda_2} = 1$ and $\varepsilon_{\lambda_1}/\varepsilon_{\lambda_2} = 0.75$.

The thermomechanical characteristics of the PFCs change dramatically with the plasma interaction and these modifications have consequences on the characteristic time evolution of the heat diffusion in the layers and/or bulk of the material. The proposed method relies on a ratio of measurement to eliminate the temperature variation introduced. As a consequence the modifications of the surface of the PFC does not affect at all the principle of the measurement. It is worth noting that the modifications of the PFC surface and characteristics are not a problem for the surface temperature measurement, using the proposed method and/or the classical IR pyrometry. However, this is a clear difficulty for the estimation the heat flux interacting with the surface and leading to the measured temperature. Indeed, the estimation of this heat flux relies on both a structure (semi-infinite, layers...) for the PFC and a surface temperature. Since the structure of the material changes the associated modelling to 'invert' the measured temperature becomes more difficult and the heat flux estimation is less accurate; this is independent of the method used to determine the surface temperature.

5. Conclusions

In future fusion devices, the PFCs will be mainly made of metallic materials like beryllium and tungsten. The surface temperature measurements will be essential for the global understanding of the plasma wall interaction as well as for safety reasons. Moving from carbon with high emissivity to materials with low emissivity results in an enhanced contribution of the reflected flux to the collected flux by the detector. The pulsed photothermal method allows a measurement of the surface temperature independently of the reflected flux and of the parasitic flux (Bremsstrahlung) independently of the wavelength detection range. This method represents a clear advantage for surface temperature measurement not only in presence of strong reflected flux, but also when dramatic variation of emissivity occurs like for beryllium which emissivity dramatically drops by a factor of 5 when melting. From this analysis, it is shown that the typical time width of the measurement can be triggered over less than 10 μs after the pulsed laser and integrated over a period of 1–3 μs with the assumption that in this time window (between the laser pulse and the final detection)

the hot spots possibly induced by the laser pulse (non-uniform surface temperature) have cooled down and that the surrounding remains in steady state. Therefore, this method can possibly allow for a time resolution of the ELMs and the disruptions. Finally, it is shown that the detection in the wavelength range from 1.1 to 1.6 μm presents several significant advantages in terms of time constant and price and that InGaAs detectors appear well adapted to this purpose.

References

[1] A. Lioure, J. Paméla, A. Kaye, et al., Fusion Eng. Design 74 (2005) 141.
[2] R. MitteauTore Supra Team, J. Nucl. Mater. 337–339 (2005) 795.
[3] T. Eich, A. Herrmann, P. Andrew, et al., J. Nucl. Mater. 313–316 (2003) 919.
[4] P. Andrew, P. Coad, T. Eich, et al., J. Nucl. Mater. 313–316 (2003) 135.
[5] R. Reichle, C. Pocheau, E. Delchambre, et al., J. Nucl. Mater. 313–316 (2003) 711.
[6] D. Hernandez, Rev. Sci. Instr. 76 (2005) 1.
[7] P. Saunders, in: J. F Dubbeldam, M J de Groot (Eds.), Proceedings of TEMPMEKO 99, 7th International Symposium on Temperature and Thermal Measurements in Industry and Science, IMEKO/NMi Van Swinden Laboratorium, Delft, 1999, p. 631.
[8] T. Loarer, J.J. Greffet, M. Huetz-Aubert, Appl. Opt. 29 (7) (1990) 979.
[9] T. Loarer, J.J. Greffet, Appl. Opt. 31 (25) (1992) 5350.
[10] A. Lothon, Pyrométire photothermique impulsionnelle à fibre optiques, Application à la mesure de la température des aubages mobiles des turbines à vapeur d'EDF, Thèse de Doctorat Ecole Centrale, Paris 1993.
[11] O. Eyal, V. Scharf, A. Katzir, Appl. Opt. 37 (25) (1998) 5945.
[12] A. Hermann, Private communication on surface temperature measurements in ASDEX Upgrade.
[13] G. Federici, C. Skinner, J.N. Brooks, et al., Nucl. Fusion 41 (12R) (2001) 1967.
[14] E. Delchambre, R. Reichle, R. Mitteau, et al., J. Nucl. Mater. 337–339 (2005) 1069.
[15] H.-D. Falter, High heat flux exposure tests on 10 mm BE tiles brazed to an actively cooled vapotron, made from CuCrZr, JET Report JET-R(96)02, March 1996.